Optimum Burn Scheduling for Low-Thrust Orbital Transfers

R. G. Melton,* K. M. Lajoie,† and J. W. Woodburn†
Pennsylvania State University, University Park, Pennsylvania

This paper describes a method for optimizing the point at which thrust should be initiated on each passage of a low-thrust, multiple finite-duration perigee-burn ascent trajectory, with the thrust vector always oriented perpendicular to nadir. The quantity being minimized is the rotation of the line of apsides. The semianalytic method developed here requires only a simple root-finding routine for the numerical portion of the solution. A perturbation solution (two-variable expansion) is used to model the flight path during the burn, yielding a "burn-on" position with a maximum error of approximately 2%.

Nomenclature

b_k	= Tschebycheff coefficients
b_{3k}	= Fourier coefficients
d_i	= Taylor series coefficients
e	= eccentricity
F_0	= total thruster force
f_r	= radial fraction of thrust force
f_t	= transverse fraction of thrust force
G	= gravitational constant
g_0	= gravitational acceleration at sea level
I_{sp}	= specific impulse
M	= mass of the Earth
$M_{s/c}$	= spacecraft mass
m	= dimensionless spacecraft mass
p	= semilatus rectum
$Q(\theta_B)$	= characteristic function whose root is the optimum burn-on point
R	= radial position of spacecraft
r	= dimensionless radial position
T	= time
T_n	= Tschebycheff polynomial
t	= dimensionless time
t_B	= duration of burn
u	= total solution to perturbed motion, $= 1/r$
β	= arc length of burn
δ	= rotation of the line of apsides
ε	= perturbation parameter
θ	= true anomaly (angular position)
ξ	= dimensionless inverse of angular momentum
ω	= argument of perigee

Superscripts

$(\ )'$	= derivative with respect to θ
$\tilde{(\ )}$	= slowly varying parameters
$(\ )^*$	= optimum point

Subscripts

i	= initial condition
0	= unperturbed (Keplerian) portion of the solution
1	= perturbed portion of solution

Introduction

FOR low-thrust, multiple perigee-burn ascents, one of the principal optimization problems is that of minimizing the propellant required for the transfer [usually from low-Earth orbit (LEO) to geosynchronous-Earth orbit (GEO)]. This requires a compromise between impulsive burns (with minimum propellant usage, but high accelerations) and burns of finite duration (with inefficient use of propellant, due to what Robbins[1] called "velocity losses"). A typical mission would consist of a number of finite perigee burns (low thrust), with a single "impulsive" burn at apogee (generally resulting in a relatively low acceleration) to effect the plane change and circularize the trajectory at GEO. (Examples are given in Refs. 2 and 3.)

A significant problem arises if the finite burns are not timed so as to maintain a fixed argument of perigee (i.e., a stationary line of apsides for the set of transfer ellipses). The result would be an apogee on the final transfer ellipse that did not lie on the geosynchronous orbit. (An alternative is to center the burn arcs at perigee, resulting in a relatively simple thrust controller, but requiring ground station intervention to command trim burns that correct for the rotated position of perigee. See, for example, Ref. 4.) While some trim maneuvers would probably be inevitable for other reasons,[3] the extra propellant needed to correct the apogee position in this case alone would be significant. This paper presents a simple analytic approximation that specifies the location at which each finite burn should be initiated in order to minimize the rotation of the line of apsides. The analysis is limited to those missions using transverse thrusting (i.e., the thrust vector is directed normal to the radial direction and in the orbital plane), although the method employed could be extended to other simple steering strategies.

Redding and Breakwell[5] and Redding[6] have examined the relations among gravity losses, number of perigee burns, and transfer time, employing a variational approach and use of the primer vector formulation to optimize low-thrust trajectories. Edelbaum et al.[7] also examined generalized optimal low-thrust ascent trajectories. Some of the numerical optimization studies include work by Vulpetti[8] and Adams.[9]

Brodksy[10] describes a trade study on low-thrust vs impulsive-burn ascents, with particular attention to the advantage of simple steering laws. Kaplan and Yang[11] examined a number of simple steering strategies for low-thrust, multiple-burn ascents, concluding that transverse thrust was the optimum if the thrust direction were fixed relative to the vehicle. Such a steering geometry does not minimize propellant usage, but the propellant penalty is not severe.[5] Under the assumption of transverse-thrust steering, the work described here results in a method for optimizing burn scheduling in the sense that an onboard controller, using relatively elementary calculations, could manage an ascent more autonomously than those requiring ground station commands for corrective trim burns.

Presented as Paper 86-2010 at the AIAA/AAS Astrodynamic Conference, Williamsburg, VA, Aug. 18–20, 1986; received June 5, 1986; revision received July 20, 1987.

*Associate Professor of Aerospace Engineering. Senior Member AIAA.
†Student, Department of Aerospace Engineering. Student Member AIAA.

Flight-Path Model

Following the method presented by Everett et al.,[12] the equations of motion are solved via the first-order perturbation method of multiple-variable expansions. The method is summarized subsequently but diverges from that of the previous reference in order to make the optimization tractable.

Equations of Motion

Beginning with the differential equations of motion in polar form

$$M_{s/c}\left[\frac{d^2R}{dT^2}-R\left(\frac{d\theta}{dT}\right)^2\right]=\frac{-GMM_{s/c}}{R^2}+F_0f_r \tag{1}$$

$$M_{s/c}\left[R\frac{d^2\theta}{dT^2}+2\frac{dR}{dT}\frac{d\theta}{dT}\right]=F_0f_t \tag{2}$$

$$\dot{M}_{s/c}=\frac{-F_0}{I_{sp}g_0} \tag{3}$$

where $M_{s/c}$ is the mass of the spacecraft, R the radial position, θ the true anomaly, G the gravitational constant, M the mass of the Earth, F_0 the total thruster force, f_r and f_t the fractions of thrust in the radial and transverse directions, respectively, I_{sp} the specific impulse of the thruster, and g_0 the gravitational acceleration at sea level, use of the substitutions

$$R=R_ir \tag{4}$$

$$T=(R_i^3/GM)^{1/2}t \tag{5}$$

$$M_{s/c}=M_im \tag{6}$$

$$\varepsilon=\frac{F_0}{GMM_i/R_i^2} \tag{7}$$

$$\lambda=\left(\frac{GM}{R_iI_{sp}^2g_0^2}\right)^{1/2} \tag{8}$$

renders the formulation dimensionless. The characteristic length R_i is taken to be the radial position at perigee of the initial orbit, and M_i the initial spacecraft mass; ε is the perturbation parameter ($\varepsilon \ll 1$ for low-thrust maneuvers). In the remainder of the analysis, the quantity f_r is set to zero under the condition of purely transverse thrusting.

The familiar substitution

$$u=1/r \tag{9}$$

and the notation $(') = d/d\theta$ yield the equations

$$u''+u-u^4t'^2=-(\varepsilon/m)ut'^2u'f_t \tag{10}$$

$$(u^2t')'=-(\varepsilon/m)u^3t'^3f_t \tag{11}$$

$$m'=-t'\lambda\varepsilon \tag{12}$$

the first two of which are weakly nonlinear but can be linearized via the substitution

$$\xi=u^2t' \tag{13}$$

where ξ is the dimensionless inverse of the vehicle's angular momentum per unit mass.

Two-Variable Expansion

With $\varepsilon \ll 1$, it is assumed that the function u varies with θ approximately, as in a Keplerian orbit, but that the perturbation caused by the low-level thrust creates an additional term in u that varies rather slowly, i.e., as a function of $\tilde{\theta}=\varepsilon\theta$. This is the basis for the two-variable expansion method.[13–15] Retaining only first-order terms in ε, the solutions to Eqs. (10–13) are

$$u(\theta,\varepsilon)=u_0(\theta,\tilde{\theta})+\varepsilon u_1(\theta,\tilde{\theta})+O(\varepsilon^2) \tag{14}$$

$$t'(\theta,\varepsilon)=v_0(\theta,\tilde{\theta})+\varepsilon v_1(\theta,\tilde{\theta})+O(\varepsilon^2) \tag{15}$$

$$\xi(\theta,\varepsilon)=\xi_0(\theta,\tilde{\theta})+\varepsilon\xi_1(\theta,\tilde{\theta})+O(\varepsilon^2) \tag{16}$$

$$m(\theta,\varepsilon)=m_0(\theta,\tilde{\theta})+\varepsilon m_1(\theta,\tilde{\theta})+O(\varepsilon^2) \tag{17}$$

where the terms with zero subscripts are the unperturbed (Keplerian) terms. Substituting into Eqs. (10–13) and equating like powers of ε yields

$$u_0(\theta,\tilde{\theta})=[1+e\cos(\theta-\omega)]/p \tag{18}$$

$$p=a_0(1-e_0^2)/R_0 \tag{19}$$

$$v_0(\theta,\tilde{\theta})=p^{3/2}/[1+e\cos(\theta-\omega)]^2 \tag{20}$$

$$\xi_0=u_0^2v_0=p^{-1/2} \tag{21}$$

$$\frac{\partial\xi_1}{\partial\theta}=\frac{-u_0^3v_0^3}{m}f_t \tag{22}$$

where all zero subscripts indicate unperturbed (pre–burn) quantities. After considerable algebra, the key relations produced are

$$u_1''+u_1=\frac{-2e}{p}\frac{\partial\omega}{\partial\tilde{\theta}}\cos(\theta-\omega)+\frac{2}{p}\frac{\partial e}{\partial\tilde{\theta}}\sin(\theta-\omega)-\frac{2e}{p^2}\frac{\partial p}{\partial\tilde{\theta}}\sin(\theta-\omega)+\frac{2\xi_1}{p^{1/2}}+\frac{ep\sin(\theta-\omega)}{m[1+e\cos(\theta-\omega)]^3} \tag{23}$$

and

$$\frac{\partial\xi_1}{\partial\theta}=\frac{-f_tp^{3/2}}{m[1+e\cos(\theta-\omega)]^3} \tag{24}$$

A highly accurate approximation of the cubic term in these last expressions yields flight paths of high accuracy also, but their mathematical form is not amenable to optimization other than by a purely numerical method. Therefore, we seek an approximate analytic solution to Eq. (23) that *need not model the flight path* to any particular degree of precision but which should provide accurate estimates of the optimum burn-on point.

Cubic Term Expansions

While Everett et al.[12] showed that accurate flight paths are generated by using Fourier or Tschebycheff expansions of the cubic term

$$[1+e\cos\theta]^{-3}=\frac{b_{30}}{2}+\sum_{k=1}^{\infty}b_{3k}\cos k(\theta-\omega) \tag{25}$$

or

$$[1+e\cos\theta]^{-3}=\frac{b_0}{2}+\sum_{k=1}^{\infty}b_kT_k(\cos(\theta-\omega)) \tag{26}$$

the forms of the flight-path models were too cumbersome for optimization. Retaining only first-order terms in either expansion reduces the complexity of the flight-path model but decreases its accuracy considerably.

Alternatively, first-order expansions of the cubic term using Taylor series or the binomial theorem yield quite adequate results over the range of θ that is required. Figure 1 shows a

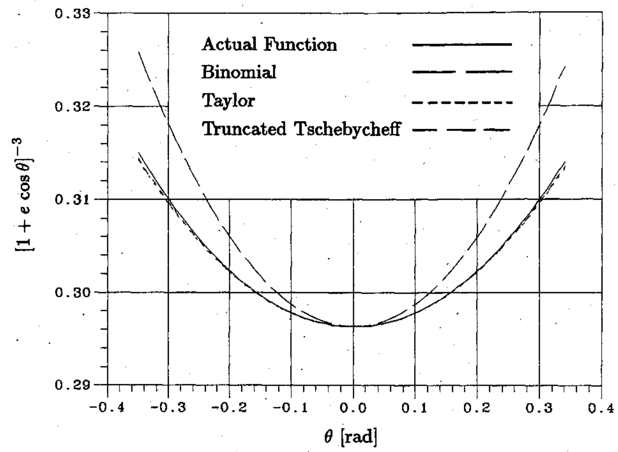

Fig. 1 First-order expansions of the cubic term $[1+e\cos\theta]^{-3}$, for $e=0.5$.

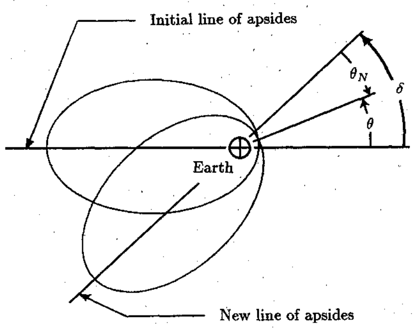

Fig. 2 Rotation of the line of apsides.

comparison of these representations of the cubic term, including Taylor series, binomial expansion, and a special form of Tschebycheff series[16] intended to give better convergence when the series is truncated. The value of eccentricity used is $e = 0.5$. Of these, the Taylor series has the simplest form, and is found to be

$$[1+e\cos(\theta-\omega)]^{-3} \approx \mathrm{d}_0 + \mathrm{d}_1\cos(\theta-\omega) \tag{27}$$

with

$$\mathrm{d}_0 = \frac{1}{(1+e)^3} + \frac{3e}{(1+e)^4} \tag{28}$$

and

$$\mathrm{d}_1 = \frac{-3e}{(1+e)^4} \tag{29}$$

Direct integration of Eq. (24) yields

$$\xi_1 = \frac{-p^{3/2}f_t\mathrm{d}_0}{m}(\theta-\omega) - \frac{p^{3/2}f_t\mathrm{d}_1}{m}\sin(\theta-\omega) + g(\bar{\theta}) \tag{30}$$

where $g(\bar{\theta})$ is to be determined from boundary conditions.

One final approximation is required to allow integration of Eq. (23). As described in Ref. 12, the linear term in $(\theta-\omega)$ can be replaced by a sinusoidal form that is approximately linear over the range of interest in order to simplify the integration (although the method of variation of parameters would not require that substitution); however, in the present work, it was found that the optimization becomes intractable if all terms in Eq. (23) are not sinusoidal. Consequently, Eq. (30) becomes

$$\xi_1 = \frac{-p^{3/2}f_t}{m}(\mathrm{d}_0+\mathrm{d}_1)\sin(\theta-\omega) + g(\bar{\theta}) \tag{31}$$

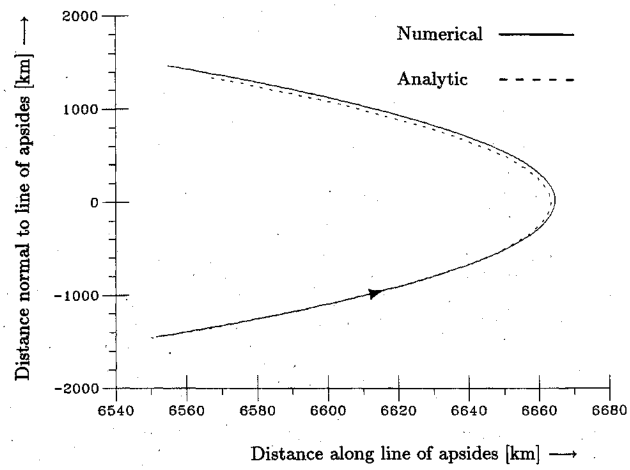

Fig. 3 Flight-path comparison for test case 1 (origin at Earth's center).

The function of integration $g(\bar{\theta})$ must satisfy the boundary condition

$$\xi_1|_{\theta=\theta_B} = 0 \tag{32}$$

where θ_B is the true anomaly at "burn-on," yielding

$$g(\bar{\theta}) = \frac{p^{3/2}f_t}{m}(\mathrm{d}_0+\mathrm{d}_1)\sin(\theta_B-\omega) \tag{33}$$

Substituting Eqs. (31) and (33) into Eq. (23), and integrating the latter using variation of parameters, gives the perturbed part of the flight-path equation

$$u_1 = \frac{-epd_1}{3m}\sin\theta\cos\theta + g_1(\theta) - C_1\cos\theta + C_2\sin\theta \tag{34}$$

with

$$g_1(\bar{\theta}) = 2g(\bar{\theta})p^{1/2} \tag{35}$$

$$C_1 = \frac{-epd_1}{3m}\sin\theta_B^3 + g_1(\bar{\theta})\cos\theta_B \tag{36}$$

$$C_2 = \frac{epd_1}{3m}\cos\theta_B^3 - g_1(\bar{\theta})\sin\theta_B \tag{37}$$

Optimization of θ_B

Minimization of δ, the rotation of the line of apsides, is the optimization criterion. Referring to Fig. 2, this quantity can be expressed as

$$\delta = \theta - \theta_N \tag{38}$$

where θ is the true anomaly at the "burn-off" point, measured relative to the original line of apsides, and θ_N the true anomaly of the same point, but measured relative to the new line of apsides. The substitution

$$\theta = \theta_B + \beta \tag{39}$$

where β is the arc length of the burn, makes Eq. (38) an explicit function of θ_B. Values of β can be estimated using Kepler's time equation as follows: For a given burn duration t_B, and assuming approximately Keplerian orbits starting at perigee, the change in eccentric anomaly (and, hence, that of the true anomaly) can be generated with errors in β of less than 2% (for values of eccentricity up to 0.7).

Optimization of the burn consists of determining θ_B so as to make

$$\theta \approx \theta_N \tag{40}$$

Using the orbital parameters at the end of the burn, the new true anomaly is

$$\theta_N = \cos^{-1}\left[\frac{1}{e}\left(\frac{u}{\xi^2} - 1\right)\right] \tag{41}$$

The eccentricity of the perturbed orbit can be expressed as

$$e = \left\{1 + \frac{1}{\xi^4}\left[\left(\frac{\partial u}{\partial \theta}\right)^2 + u^2\right] - \frac{2u}{\xi^2}\right\}^{1/2} \tag{42}$$

Finally, combining Eqs. (38–42) gives the function $Q(\theta_B)$, whose root in the perigee region is the optimum burn-on true anomaly θ_B^*.

Results

Flight-Path Comparisons

The simplified flight-path model that results from the Taylor expansion of the cubic term has been compared with numerical integrations of the exact differential equations for several test cases, two of which are presented here. These results are discussed before proceeding to the optimization problem.

Test Case 1

This case represents a spacecraft whose thrust level is in the upper region for low-thrust spacecraft. The parameters for test case 1 are

$$e_0 = 0.41369$$
$$R_0 = 6663 \text{ km}$$
$$F_0 = 3117 \text{ N}$$
$$M_{s/c} = 5875 \text{ kg}$$
$$I_{sp} = 300 \text{ s}$$
$$\theta_B = -0.219 \text{ rad}$$
$$t_B = 317 \text{ s}$$

Results of this comparison with numerical simulations are shown in Fig. 3. The error in the flight path is seen to increase toward the burn-off point, but the final error in radial position is less than 1%.

Test Case 2

This case indicates the applicability of the flight-path model to missions having somewhat larger acceleration levels than would be employed for LEO-to-GEO transfers. In addition, the initial eccentricity is larger than in the previous test cases and has a value typical of that for the last segment of a multiple-burn ascent to GEO. The parameters are

$$e_0 = 0.6$$
$$R_0 = 6600 \text{ km}$$
$$F_0 = 2500 \text{ N}$$
$$M_{s/c} = 3500 \text{ kg}$$
$$I_{sp} = 300 \text{ s}$$
$$t_B = 250 \text{ s}$$

Figure 4 shows the comparison with numerical results. The error in radial position at burn-off is still within 1%.

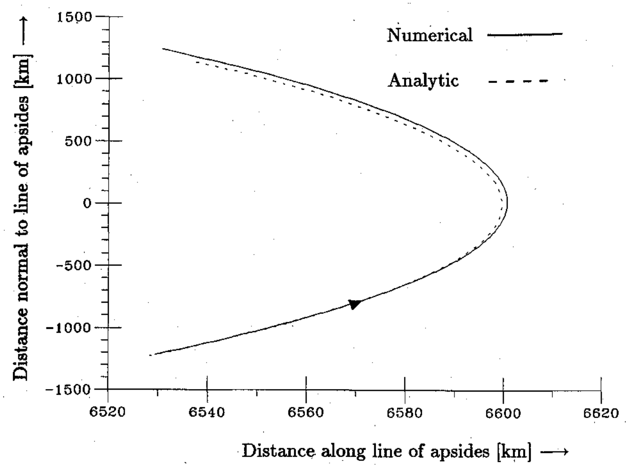

Fig. 4 Flight-path comparison for test case 2 (origin at Earth's center).

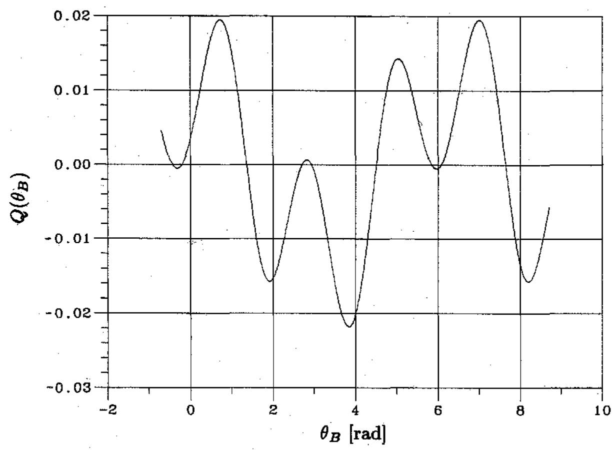

Fig. 5 Optimization function for test case 1.

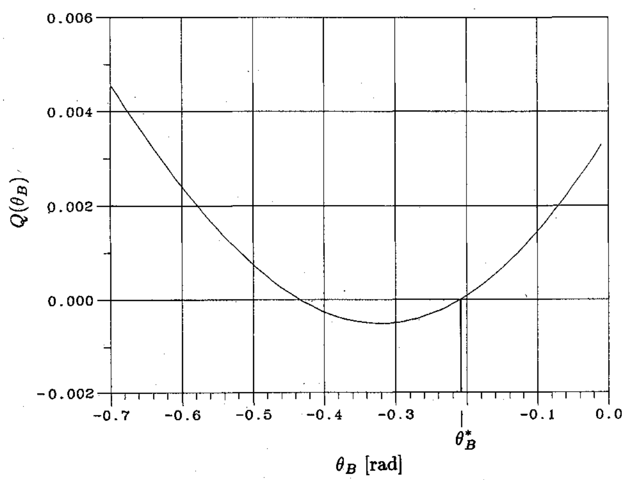

Fig. 6 Expanded plot of $Q(\theta_B)$ for case 1.

Optimized Trajectory Comparisons

For each of the test cases, the function $Q(\theta_B)$ was generated over a 3π interval. The region of interest about perigee was then plotted on an expanded scale to determine the optimum burn-on true anomaly and the result compared with that obtained from numerical integrations of the exact differential equations (iterated to obtain θ_B^*).

Figures 5–7 show the optimization results for test case 1. The function $Q(\theta_B)$ has a period of 2π and contains multiple roots,

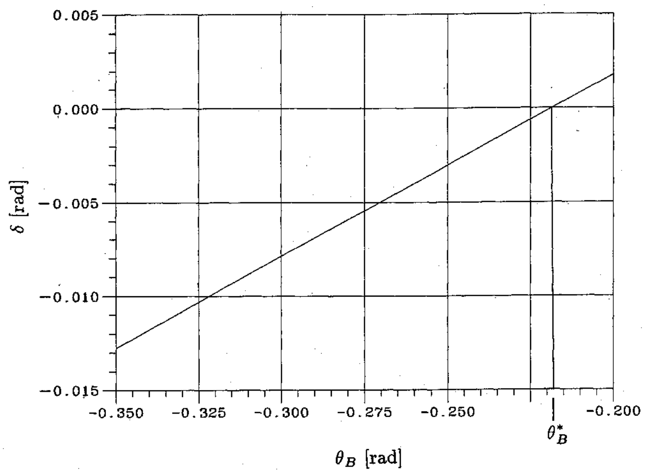

Fig. 7 Numerical solution for θ_B^* (case 1).

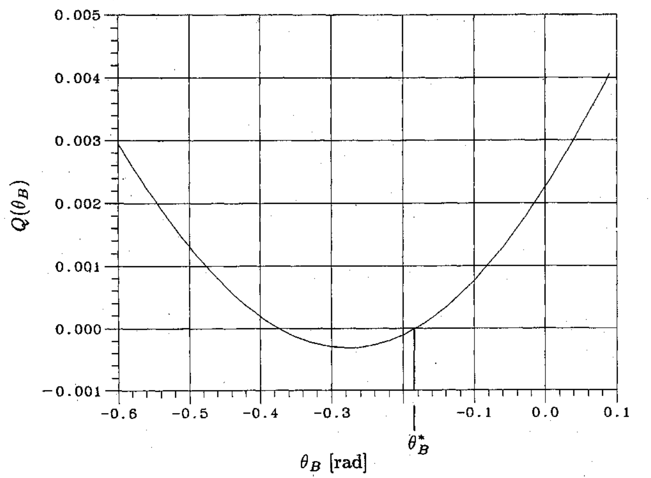

Fig. 8 Optimization function for test case 2.

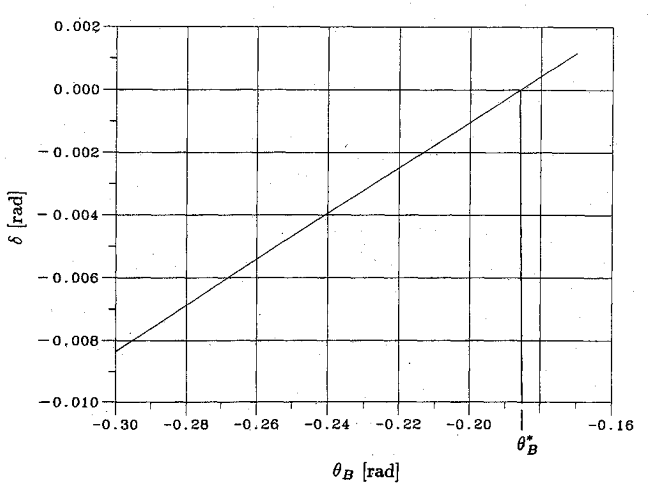

Fig. 9 Numerical solution for θ_B^* (case 2).

Table 1 Comparison of test cases

Case	θ_B^*, rad Analytic	Numerical	Error (relative), %	δ, deg
1	−0.220	−0.219	0.46	0.0088
2	−0.182	−0.186	2.15	0.0170

as seen in Fig. 5. One of the roots near the value $\theta_B = \pi$ corresponds to an apogee burn, which is not of interest here. Note that there are three other roots within the first 2π interval of θ_B: one of these, near perigee, is the optimum burn-on point, the other two (near perigee and apogee) are false roots that appear as a consequence of the approximations employed in the perturbation solution for the flight-path model. Intuition dictates that the rotation of the line of apsides should be a monotonic function of the burn-on point; therefore, only one root of $Q(\theta_B)$ in the perigee region is physically meaningful.

Analysis of the test cases indicates that the correct root near perigee is always at the point where the function $Q(\theta_B)$ crosses the abscissa axis from negative to positive. This is purely an "empirical" observation of a numerical experiment; further analysis will be required to determine the cause.

A comparison of the root locations is provided in Figs. 6 and 7, which show, respectively, $Q(\theta_B)$ and δ (computed numerically). Ideally, the curve in Fig. 6 would be shifted to the right and up, making it tangent to the abscissa axis at the one true root of $Q(\theta_B)$. In test case 1, the error in optimum burn-on location θ_B^* is approximately 0.46%, which would translate into a rotation of the line of apsides of 0.0088 deg. The optimization results of both test cases are presented in Table 1, with the corresponding plots shown in Figs. 6–9. It should be noted that the maximum error encountered in θ_B^* is approximately 2.2%, but that it is associated with the high acceleration level of test case 2. Other test cases showed good results as well. The method is thus validated over the range of orbital and vehicle parameters of interest in low-thrust ascent trajectories.

Conclusions

A first-order expansion of nonlinear terms in the differential equations of motion leads to a favorable approximation of the flight path, as well as providing a solution amenable to simple optimization. While the flight-path model shows decreasing accuracy over the length of the burn, it remains within 1% of the numerical solution.

The optimization procedure consists of generating a relatively simple function of the known propulsion and orbital parameters, and extracting the one root of physical significance of this function, which gives the optimum burn-on true anomaly. An empirical method for identifying that root has been described, but no rigorous justification is available as yet. A worst-case analysis indicates that the maximum error in this optimization is on the order of 2%. Although graphical methods were used in this work to determine the root of interest, the entire procedure could be implemented numerically in a code that executes on a vehicle's onboard computer. Computationally intensive numerical simulations for determining the optimum burn-on point could thus be replaced by simple root-finding calculations.

Acknowledgments

The authors wish to thank the Department of Aerospace Engineering and the Engineering Computer Laboratory of The Pennsylvania State University for their support in conducting this work and in preparing this manuscript.

References

[1]Robbins, H. M., "An Analytic Study of the Impulsive Approximation," *AIAA Journal*, Vol. 4, Aug. 1966, pp. 1417–1423.

[2]Hoge, S. L., and Oh, I-H., "ERBS Orbit Ascent Utilizing Continuous Low Thrust Maneuvers," AAS Paper 85-303, AAS/AIAA Astrodynamics Specialist Conference, Vail, CO, Aug. 1985.

[3]Adams, N. J., and Melton, R. G., "Orbital Transfer Error Analysis for Multiple, Finite Perigee Burn, Ascent Trajectories," *Journal of the Astronautical Sciences*, Vol. 34, Oct.–Dec. 1986, pp. 355–373.

[4]Wertz, J. R., Mullikin, T. L., and Brodsky, R. F., "Reducing the Cost and Risk of Orbit Transfer," AIAA Paper 87-0172, Jan. 1987.

[5]Redding, D. C. and Breakwell, J. V., "Optimal Low-Thrust Transfers to Synchronous Orbit," *Journal of Guidance, Control, and Dynamics*, Vol. 7, No. 2, March–April 1984, pp. 148–155.

[6]Redding, D. C., "Highly Efficient, Very Low-Thrust Transfers to Geosynchronous Orbit: Exact and Approximate Solutions," *Journal of Guidance, Control, and Dynamics*, Vol. 7, No. 2, March–April 1984, pp. 141–147.

[7]Edelbaum, T. M., Sackett, L. L., and Malchow, H. L., "Optimal Low Thrust Geocentric Transfer," AIAA Paper 73-1074, Oct. 1973.

[8]Vulpetti, G., "A Non-Variational Approach to Multiple Finite Burn Propellant Optimization," IAF Paper 84-354, XXXV Congress of the International Astronautical Federation, Lausanne, Switzerland, Oct. 1984.

[9]Adams, N. J., "Error Analysis for Multiple, Finite-Burn Ascent Trajectories," Master's Thesis, Dept. of Aerospace Engineering, The Pennsylvania State Univ., University Park, PA, Jan. 1984.

[10]Brodsky, R. F., "An Economical and Flexible Alternative Orbital Transfer Vehicle," IAF Paper 81-16, XXXII Congress of the International Astronautical Federation, Rome, Italy, Sept. 1981.

[11]Kaplan, M. H. and Yang, W., "Finite Burn Effects on Ascent Stage Performance," AAS Paper 81-153, AAS/AIAA Astrodynamics Specialist Conference, Lake Tahoe, NV, Aug. 1981.

[12]Everett, K. A., Adams, N. J., and Melton, R. G., "First-Order Perturbation Analysis for Low-Thrust Spacecraft," AAS Paper 85-442, AAS/AIAA Astrodynamics Specialist Conference, Vail, CO, Aug. 1985.

[13]Kevorkian, J. and Cole, J. D., *Perturbation Methods in Applied Mathematics*, Springer-Verlag, NY, 1981.

[14]Cole, J. D., *Perturbation Methods in Applied Mathematics*, Blaisdell, Waltham, MA, 1968.

[15]Bellman, R. E., *Perturbation Methods in Mathematics, Physics, and Engineering*, Holt, Rinehart, and Winston, NY, 1964.

[16]Fox L, and Parker, I. B., *Chebyshev Polynomials in Numerical Analysis*, Oxford University Press, NY, 1968.